A *Medicago truncatula* phosphate transporter indispensable for the arbuscular mycorrhizal symbiosis

Hélène Javot*, R. Varma Penmetsa†, Nadia Terzaghi†, Douglas R. Cook†, and Maria J. Harrison*‡

*Boyce Thompson Institute for Plant Research, Cornell University, Tower Road, Ithaca, NY 14850; and †Department of Plant Pathology, University of California, One Shields Avenue, Davis, CA 95616

Edited by Steven E. Lindow, University of California, Berkeley, CA, and approved December 5, 2006 (received for review September 15, 2006)

The arbuscular mycorrhizal (AM) symbiosis is a mutualistic endosymbiosis formed by plant roots and AM fungi. Most vascular flowering plants have the ability to form these associations, which have a significant impact on plant health and consequently on ecosystem function. Nutrient exchange is a central feature of the AM symbiosis, and AM fungi obtain carbon from their plant host while assisting the plant with the acquisition of phosphorus (as phosphate) from the soil. In the AM symbiosis, the fungus delivers P_i to the root through specialized hyphae called arbuscules. The molecular mechanisms of P_i and carbon transfer in the symbiosis are largely unknown, as are the mechanisms by which the plant regulates the symbiosis in response to its nutrient status. Plants possess many classes of P_i transport proteins, including a unique clade (Pht1, subfamily I), members of which are expressed only in the AM symbiosis. Here, we show that MtPT4, a *Medicago truncatula* member of subfamily I, is essential for the acquisition of P_i delivered by the AM fungus. However, more significantly, MtPT4 function is critical for AM symbiosis. Loss of MtPT4 function leads to premature death of the arbuscules; the fungus is unable to proliferate within the root, and symbiosis is terminated. Thus, P_i transport is not only a benefit for the plant but is also a requirement for the AM symbiosis.

biotrophic | membrane | mineral nutrition | mutualism | root

Plants and their arbuscular mycorrhizal (AM) fungal symbionts have coexisted for >400 million years (1), and the association is widespread in terrestrial ecosystems. AM symbiosis provides multiple benefits for the plant, not only enhanced phosphorus and nitrogen nutrition but also tolerance to pathogens and abiotic stresses (2, 3). For AM fungi, formation of a symbiosis is an obligate requirement. Their large spores contain reserves sufficient to support growth of a hyphal germ tube, but they must form an association with a plant to acquire additional carbon to complete their life cycle (4). Development of symbiosis, in particular intraradical development of the fungus in the root cortex, is reduced if P_i availability is high (5–7). This suggests that the plant has a mechanism of regulating fungal growth, presumably to avoid the unnecessary allocation of carbon resources. The molecular basis is unknown but could occur by the control of carbon allocation (8).

In the AM symbiosis, the fungal hyphae grow through the intercellular spaces of the root and subsequently invade the inner cortical cells, developing branched hyphae, called arbuscules, within the cells (9, 10). As each arbuscule forms, the plant cell envelops it in a membrane, the periarbuscular membrane, and the result is an extensive plant–fungal interface specialized for nutrient exchange (11–14). It is predicted that P_i and carbon transfer occur at the arbuscule/cortical cell interface, although direct evidence for carbon transfer at this location is lacking (14). Current data suggest that P_i is translocated through the AM fungal hyphae as polyphosphate (polyP), and after hydrolysis, in the arbuscule, P_i is exported from the AM fungus to the periarbuscular space (15–17). The import of P_i across the periarbuscular membrane, into the root cell is then mediated by plant transporters. Currently, two classes of P_i transporters are implicated in P_i transport in AM symbiosis: mycorrhiza-induced P_i transporters of Pht1, subfamily III; and mycorrhiza-specific P_i transporters of Pht1, subfamily I. Members of subfamily III, such as StPT3 of potato, ZEAma;Pht1;6 of maize, and LjPT3 of *Lotus japonicus*, are expressed in roots but show increased expression in symbiosis (18–21). Partial down-regulation of LjPT3 reduced symbiotic P_i transfer ≈2-fold, indicating that this transporter contributes to the symbiotic P_i transport process (21). By contrast, members of subfamily 1, such as OsPT11 of rice, MtPT4 of *M. truncatula*, and LePT4 of tomato, are expressed exclusively in AM symbiosis (19, 22, 23), and their functions have not been described. All plants examined, except for *Arabidopsis*, a nonmycorrhizal plant species, possess at least one transporter in this subfamily. However, there is variation between plant species; rice contains one subfamily I P_i transporter (22), whereas potato and tomato each have two; and in tomato, it is proposed that they are functionally redundant (19). MtPT4, a member of subfamily I, is located in the periarbuscular membrane of *M. truncatula*, further suggesting a role in symbiotic P_i transfer (23).

Using both transgenic lines in which MtPT4 is down-regulated by RNAi and MtPT4 loss-of-function mutants identified by target-induced local lesions in genomes (TILLING), we demonstrate that MtPT4 is essential for symbiotic P_i transport and development of AM symbiosis.

Results and Discussion

MtPT4 Is Required for Enhanced P_i Content and Growth Resulting from AM Symbiosis. Transgenic *M. truncatula* plants expressing an RNAi construct designed to the 3′ end of the MtPT4 coding region were generated. In two independent transgenic lines designated MtPT4 RNAi 1 and RNAi 2, MtPT4 was effectively silenced, and MtPT4 transcripts and protein were not detectable [Fig. 1*A* and supporting information (SI) Fig. 6*A–F*]. In contrast, two other independent transformants, MtPT4 RNAi 3 and 4, showed MtPT4 transcript and protein levels comparable to those of the vector control lines (V1 and V2), indicating that silencing of MtPT4 had not occurred in these lines (Fig. 1*A*). These lines were designated RNAi 3 (ND, for non-down-regulated) and

Author contributions: H.J., R.V.P., D.R.C., and M.J.H. designed research; H.J., R.V.P., N.T., and M.J.H. performed research; H.J., R.V.P., N.T., and D.R.C. contributed new reagents/analytic tools; H.J., R.V.P., N.T., D.R.C., and M.J.H. analyzed data; and H.J. and M.J.H. wrote the paper.

The authors declare no conflict of interest.

This article is a PNAS direct submission.

Abbreviations: AM, arbuscular mycorrhizal; polyP, polyphosphate; ND, non-down-regulated; RLC, root length colonized; dpi, days postinoculation; hpi, hours postinoculation, TILLING, target-induced local lesions in genomes.

‡To whom correspondence should be addressed. E-mail: mjh78@cornell.edu.

This article contains supporting information online at www.pnas.org/cgi/content/full/0608136104/DC1.

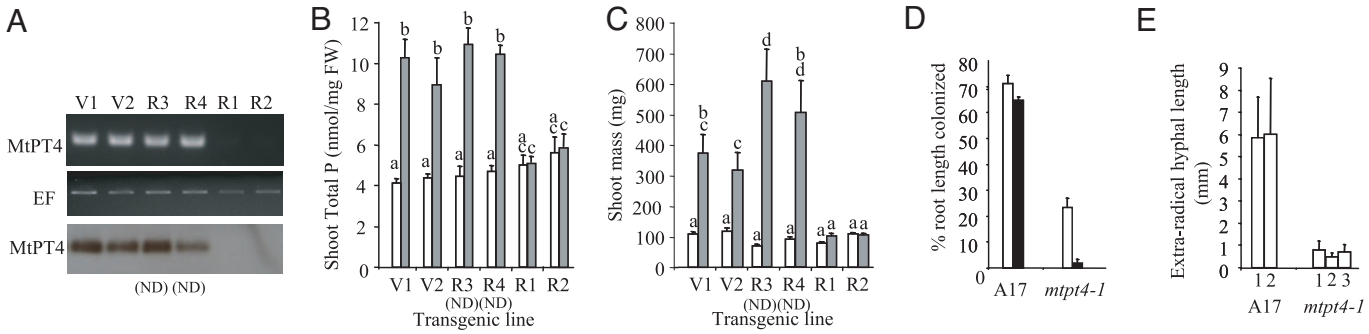

Fig. 1. Molecular and physiological analyses of the MtPT4 RNAi transgenic plants and *Mtpt4-1* mutants. (*A*) MtPT4 transcript (*Top*) and protein levels (*Bottom*) in homozygous vector control (V1 and V2) and MtPT4 RNAi transgenic lines (R 1, 2, 3, and 4) assayed by semiquantitative RT-PCR and Western blot, respectively. Plants were inoculated with *G. versiforme*. EF is an elongation factor control (*Middle*). In RNAi lines 3 and 4, MtPT4 expression was not down-regulated. Shoot P content (*B*) and shoot mass (*C*) of the transgenic plants at 72 dpi with *G. versiforme* (gray bars) or mock-inoculated controls (white bars). The mock-inoculated controls do not differ significantly from each other ($P > 0.05$). Different letters indicate lines that differ significantly from each other ($P < 0.05$). The percent RLC for each line is as follows: V1 (44 ± 1), V2 (40), R1 (12 ± 2), R2 (8 ± 4), R3 (49 ± 7), and R4 (47 ± 11). (*D*) Level of colonization of WT (A17) and *mtpt4-1* roots at 54 dpi with *G. versiforme* assessed by WGA-Alexafluor 488 staining to reveal total fungal structures (white bars) or vital staining (black bars). A17 and *mtpt4-1* differ significantly (Student's *t* test, $P < 0.0001$). (*E*) Length of live *G. versiforme* extraradical hyphae attached to roots in WT (A17) (two plants) and *mtpt4-1* (three plants). Data are the average of 16 and 10 measurements per plant for A17 and *mtpt4-1*, respectively.

RNA:4 (ND) and were used as additional controls. The region of MtPT4 targeted by the RNAi construct shares <42% identity at the nucleotide level with other phosphate transporters of the PHT1 family. Consistent with this sequence divergence, the expression of other PHT1 family members was not altered in the RNAi lines (SI Fig. 6*G*).

The transgenic plants were inoculated with an AM fungus, *Glomus versiforme*, and grown under low-P_i conditions to reveal increases in shoot P content and biomass resulting from the symbiosis. Under these conditions, the shoot P content and shoot mass of the mock-inoculated plants were similar in all transgenic lines (Fig. 1 *B* and *C*). A significant increase in shoot P levels (average increase of 230%) and shoot mass (average increase of 500%) associated with the mycorrhizal treatment was apparent in the vector and MtPT4 RNAi (ND) control plants. By contrast, MtPT4 RNAi 1 and 2 plants inoculated with *G. versiforme* did not differ significantly from their mock-inoculated controls. These data indicate that MtPT4 is required for the increase in P_i content and growth associated with AM symbiosis and suggest that other P_i transporters do not compensate for the loss of MtPT4. Furthermore, additional mycorrhiza-inducible P_i transporters, which, given their existence in other plants, are predicted to exist in *M. truncatula* also, must play a minor or different role in AM symbiosis.

Loss of MtPT4 Function Affects the Morphology and Intra- and Extraradical Growth of the AM Fungus. The root systems of these plants were analyzed to determine the extent of development of the symbiosis. The control and RNAi (ND) lines showed an average of 45% root length colonized (RLC), and fungal structures typical of the symbiosis were apparent, including intercellular hyphae, arbuscules, vesicles, and extraradical hyphae. By contrast, total fungal development in MtPT4 RNAi 1 and 2 plants was significantly lower, with only 12% and 8% RLC, respectively. In *L. japonicus*, a 1.5-fold reduction in arbuscule frequency was observed in a LjPT3 knockdown line; however, fungal morphology and development of the fungus within the root were not altered (21). In contrast, in the MtPT4 RNAi 1 and 2 plants, there was a striking difference in the morphology of the fungus relative to the controls. Arbuscules were infrequent, and those that were present were degenerating; moreover, the intercellular hyphae contained septa, which are morphological signatures of death in AM fungi (SI Fig. 7) (11, 12). This phenotype was unexpected and suggested that loss of MtPT4 function also affected development of *G. versiforme* within the root.

To confirm this, we used TILLING to identify an ethane methyl sulfonate mutant allele of MtPT4, *mtpt4-1*. *mtpt4-1* contains a G-to-A transition within a transmembrane domain-coding region, resulting in the replacement of glycine at position 172 with arginine. Structure–function analyses of transporter proteins have shown that in transmembrane domains, the replacement of noncharged residues such as glycine, with charged amino acids, leads to protein instability and loss of transport activity (24, 25). Consistent with this, MtPT4 protein was not detected in mycorrhizal roots of *mtpt4-1* (SI Fig. 8 *A–F*). Furthermore, the transport activity of the *mtpt4-1* mutant transporter protein was assayed in yeast and, although the protein is expressed, P_i transport activity was not stimulated, indicating that the mutation impacts transport activity (SI Fig. 8*G*). The *mtpt4-1* mutant is effectively a null mutant.

mtpt4-1 and WT (A17) plants were inoculated with *G. versi-*

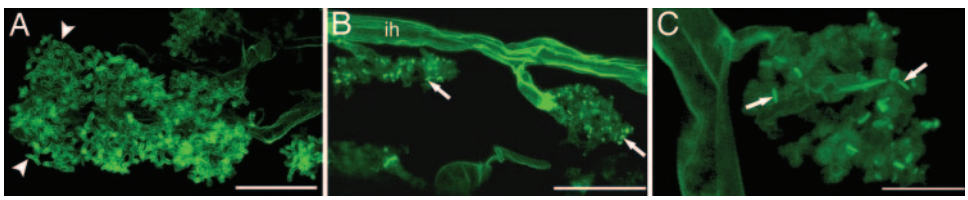

Fig. 2. Laser-scanning confocal microscope images of *G. versiforme* arbuscules in roots of *M. truncatula* WT (*A*) and *mtpt4-1* (*B* and *C*). Images are from roots at 146 hpi (taken from the experiment described in Fig. 4) but are representative of the majority of arbuscules at later time points, including 72 dpi. Roots were stained with WGA-Alexafluor 488. Arbuscules in WT are large with many full hyphal branches (arrowheads). Arbuscules in *mtpt4-1* are degenerating. Hyphal branches are indistinct, and the collapsed hyphal masses contain many septa (arrows). (Scale bars, 25 in *A* and *B* and 10 μm in *C*.) ih, intercellular hyphae.

forme, harvested at 54 days postinoculation (dpi), and stained with a vital stain followed by a cell-wall stain to evaluate both live and total fungal structures in the roots (26). In A17 roots, colonization levels assessed by cell-wall and vital staining were 71% and 65% RLC, respectively, indicating that *G. versiforme* was alive and proliferating within the roots (Fig. 1*D*). In addition, development of the extraradical hyphae was extensive (Fig. 1*E*). In contrast, in *mtpt4-1* roots, infection units were short and consisted mostly of degenerate arbuscules and septate hyphae, which were dead. Colonization levels assessed by cell-wall and vital staining were 23% and 2% RLC, respectively (Fig. 1*D*). Furthermore, extraradical hyphae did not develop (Fig. 1*E*). These data indicate that the *G. versiforme* can invade *mtpt4-1* roots, but the difference in colonization levels assessed by total and vital staining indicates that fungal growth is not sustained in the *mtpt4-1* mutant. The low colonization and collapsed arbuscule phenotypes of *mtpt4-1* (Fig. 2) are the same as those of the MtPT4 RNAi 1 and 2 lines (SI Fig. 7). Furthermore, in an F_2 population (59 individuals) derived from a cross of *mtpt4-1* and A17, the *mtpt4-1* genotype shows perfect cosegregation with the collapsed degenerating arbuscule phenotype (SI Fig. 9).

The Absence of MtPT4 Leads to the Accumulation of polyP in the Arbuscules. The classical approach to examine P_i transfer in AM symbiosis uses radioisotopes to monitor P_i delivery by the fungus (2, 27), and our initial intent was to further support the physiological studies shown in Fig. 1 with such analyses. However, during the course of the phenotypic studies, it became apparent that the mycorrhizal phenotype of the MtPT4 RNAi and *mtpt4-1* mutants was unexpectedly severe. As revealed by the experiments described in Fig. 1, growth of the fungus is not sustained in MtPT4 RNAi and *mtpt4-1* roots, and extraradical hyphae do not develop (Fig. 1*E*). Without a living extraradical mycelium in mutant lines, the results of radioisotope transfer experiments are inconclusive. As an alternative, we used polyP staining (16) to determine whether loss of MtPT4 function affected the distribution of polyP in the fungus within the root. In the cortex of vector control and A17 roots, *G. versiforme* intercellular hyphae stained strongly for polyP, whereas the arbuscules showed weak staining, consistent with the hydrolysis and export of P_i to the plant. In MtPT4 RNAi 1, RNAi 2, and *mtpt4-1* roots, *G. versiforme* intercellular hyphae, and arbuscules showed strong staining for polyP, indicating that polyP accumulates in the arbuscules in these lines (Fig. 3 and SI Fig. 10). The polyP staining patterns are consistent with the shoot P data (Fig. 1*B*) and suggest that loss of MtPT4 function results in a block in symbiotic P_i transfer from the arbuscule to the cortical cell.

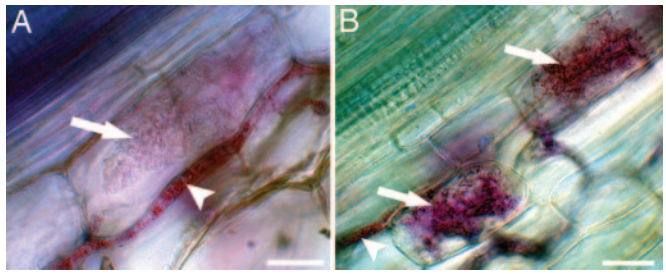

Fig. 3. Toluidine blue staining at pH 1 shows polyP as dark-red metachromatic granules in the intercellular hyphae (indicated by arrowheads) of *G. versiforme* in the V1 (*A*) and MtPT4 RNAi 2 roots (*B*). Arbuscules (indicated by arrows) stain strongly in MtPT4 RNAi 2 roots (*B*). (Scale bar, 20 μm.) Images are from roots at 28 dpi. Similar results were obtained at 4 dpi, as shown in SI Fig. 10.

MtPT4 Is Required to Maintain Arbuscule Life and to Sustain Development of the AM Fungus. The altered morphology of the arbuscules and the failure of the fungus to become established in the MtPT4 RNAi and *mtpt4-1* roots suggested a possible alteration in arbuscule development or lifespan in the mutant lines. Arbuscule development requires the differentiation of both sym-

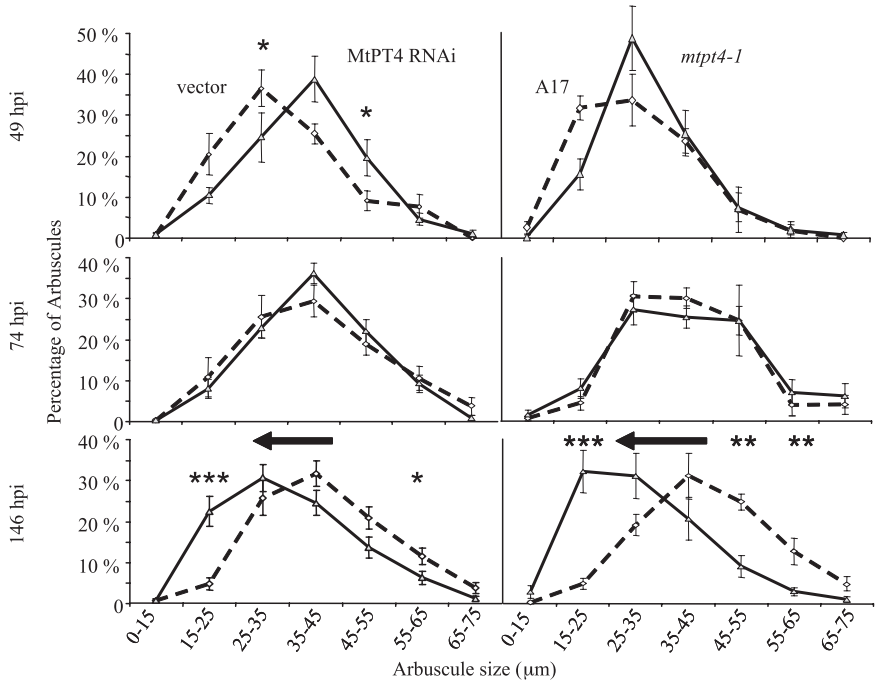

Fig. 4. Analysis of arbuscule development in *M. truncatula* RNAi lines and *mtpt4-1* inoculated with *G. versiforme*. Frequency graphs showing arbuscule size (length) distribution in arbuscule populations in vector (dotted line) and MtPT4 RNAi (solid lines) plants (*Left*) and A17 (dotted line) and *mtpt4-1* (solid line) (*Right*) at 49, 74, and 146 hpi. Asterisks indicate significant differences between the MtPT4 RNAi or *mtpt4-1* and their respective controls (***, $P < 0.0001$; **, $P < 0.01$; *, $P < 0.05$). Arrows indicate a significant shift in the arbuscule populations in MtPT4 RNAi and *mtpt4-1* plants relative to their respective controls.

bionts and is partially controlled by the plant (9). In *M. truncatula*, *G. versiforme* arbuscules develop by repeated dichotomous branching and grow until they fill the cortical cell. At some point after maturity, the arbuscules collapse, degenerate, and die. The mechanisms underlying arbuscule turnover are unknown but do not involve plant cell death. Each invaded plant cell remains alive throughout the life of the arbuscule and can host successive arbuscules (11, 12, 28). Studies of arbuscule lifespan are limited, but where examined, the lifespan is suggested to be ≈8.5 days (29). Consequently, in mycorrhizal roots, arbuscule formation and decay are ongoing, and the roots contain a population of developing and degenerating arbuscules.

To evaluate arbuscule development, MtPT4 RNAi, *mtpt4-1*, and their respective controls were inoculated with pregerminated *G. versiforme* spores that had been primed to colonize roots by preexposure to root exudates (30–32). Roots were harvested at 49, 74, and 146 h postinoculation (hpi) and 11 dpi and stained to reveal the fungus. Individual infected roots, with a distinct infection event arising from a single fungal entry point, referred to as an infection unit (11), were analyzed (SI Fig. 11). Infection unit lengths were measured and, to obtain a quantitative measure of arbuscule development, the length of individual arbuscules in the infection unit was measured. The data from the two independent vector controls (V1 and V2) and the two independent MtPT4 RNAi lines (RNAi 1 and 2) were combined. At 49 hpi, infection unit length in MtPT4 RNAi lines and *mtpt4-1* did not differ significantly from their respective controls, indicating that loss of MtPT4 does not affect the initial rate of growth of the fungus within the root cortex (SI Table 1). At 49 hpi, the populations of arbuscules in the vector and MtPT4 RNAi plants were similar, although the vector control plants showed a trend toward smaller arbuscules compared with MtPT4 RNAi plants (significant for the 25- to 35- and 45- to 55-μm size classes) (Fig. 4). Although not significant, the pattern was similar for A17 and *mtpt4-1* plants. At 74 hpi, there were no significant differences between the arbuscule populations in the vector and MtPT4 RNAi plants or in *mtpt4-1* and its respective A17 control. Relative to the 49 hpi timepoint, the median arbuscule size in all populations had increased to ≈42 μm, indicating that the arbuscules were growing. At 146 hpi, significant differences in the arbuscule populations became apparent (Fig. 4). The arbuscule populations in the vector and A17 roots showed median arbuscule sizes of 43 and 44 μm, respectively, and an increasing proportion of the population was represented in the large-size classes, indicating that the arbuscules continue to grow. In contrast, in the MtPT4 RNAi and *mtpt4-1* plants, the arbuscule populations showed a shift in the opposite direction. In each case, there was a strongly significant increase in the proportion of arbuscules in the 15- to 25-μm size class and a corresponding significant decrease in arbuscules in the 55- to 65-μm class. For *mtpt4-1*, a significant decrease in the 45- to 55-μm size class was observed also. The median size of arbuscules fell to 32 and 28 μm in the MtPT4 RNAi and *mtpt4-1* plants, respectively. Morphological analyses indicated that this shift in the arbuscule population was associated with arbuscule collapse and degeneration. Additional quantification demonstrated that, in MtPT4 RNAi and *mtpt4-1* roots, a significantly higher percentage of degenerating arbuscules was present even in the youngest regions of the infection unit (SI Table 2). To confirm that this trend was maintained, the analysis of two plant lines was further extended to 11 dpi. At 11 dpi in V1 roots, 73% of the arbuscules were represented in size classes of >35 μm. By contrast, in MtPT4 RNAi 1 roots, the arbuscule population was in significant decline, and 72% of the arbuscules were represented in size classes <35 μm (data not shown).

Although the quantitative shift in the arbuscule populations was measured at 146 hpi, qualitative differences in the arbuscules were apparent at an earlier stage. Septa, an early morphological

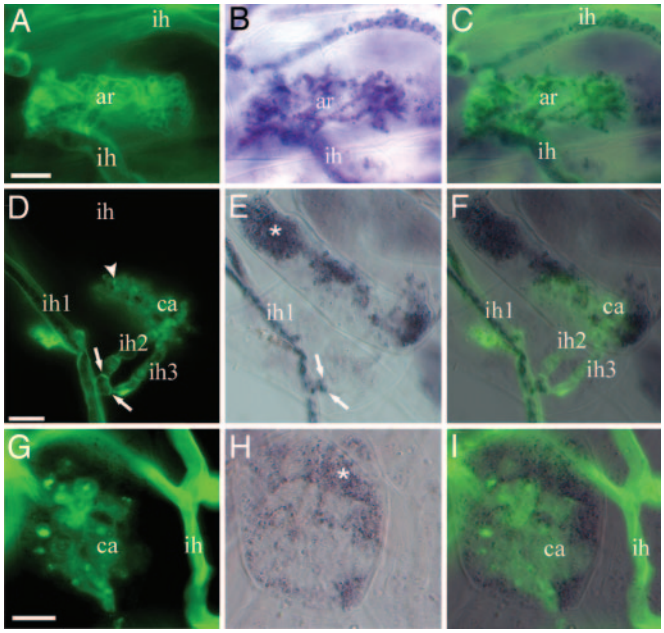

Fig. 5. Vital staining of WT and *mtpt4-1* roots colonized with *G. versiforme*. Cell-wall and vital staining reveal total fungal structures (fluorescent green staining) and living fungal structures (purple/blue precipitate), respectively. Vital staining identifies living plant cells also. Cell-wall staining (WGA-Alexafluor 488) images (*A*, *D*, and *G*) and corresponding vital stained images (*B*, *E*, and *H*). Overlay images are shown in *C*, *F*, and *I*. Images are from roots harvested at 76 hpi and 54 dpi. (*A–C*) WT root colonized with *G. versiforme* showing a live arbuscule (ar) and intercellular hyphae (ih). (*D–F*) WT root colonized with *G. versiforme* showing a collapsed arbuscule (ca) with septa (arrowhead) and subtending intercellular hyphae with septa (arrows). *, vital staining of the plant cell. Intercellular hypha (ih1) is alive but the hyphal branches (ih2 and ih3) showing septa are dead. Note that vital staining does not extend beyond the septa on hyphal branches ih2 and ih3. (*G*, *H*, and *I*) *mtpt4-1* root showing a collapsed arbuscule and dead intercellular hypha. The plant cell remains alive. (Scale bars, 10 μm.)

feature associated with arbuscule degeneration (11, 12), were visible first at 76 hpi in MtPT4 RNAi roots and 49 hpi in *mtpt4-1* roots. The phenotype in *mtpt4-1* is marginally more severe than the RNAi lines. Overall, these data indicate that, in plants lacking MtPT4, the initial development of arbuscules proceeds normally, but death of the arbuscule is triggered prematurely, as rapidly as 49 hpi, and further development of AM symbiosis cannot occur. Vital staining of WT and *mtpt4-1* roots at 76 hpi confirmed that arbuscules with turgid branches without septa were alive, whereas collapsed arbuscules containing septa were dead. Regardless of the state of the arbuscules, the invaded root cortical cells remained alive in both mutant and WT plants (Fig. 5). There are no signs of hypersensitive cell death, a typical plant strategy to eliminate an unwanted microorganisms. Therefore, the premature arbuscule collapse and death in the *mtpt4* mutants likely occur by the acceleration of the normal mechanism of arbuscule turnover, the molecular basis of which is still unknown.

Phosphate Transfer Through MtPT4 Signals the Presence of a Beneficial Fungal Symbiont. In summary, the data indicate that MtPT4, a mycorrhiza-specific P_i transporter, is required for P_i transfer in symbiosis, but more significantly, P_i transport by MtPT4 is clearly essential for AM symbiosis. Without MtPT4 function, the arbuscules die prematurely, and fungal growth is not sustained. Currently, it is unclear whether rapid death of the arbuscule is a fungal response to the local conditions, or whether it is triggered by the plant. The accumulation of polyP in the arbuscule may be toxic; however, this seems unlikely, because in WT

roots, both the extra- and intraradical hyphae can accumulate significant levels of polyP (33, 34). Alternatively, arbuscule death could be triggered by the plant, either actively by acceleration of the normal mechanism of arbuscule turnover or simply as a consequence of inadequate carbon flow from the plant. A link between carbon and phosphate exchange in AM symbiosis has not been shown directly but has received extensive discussion, particularly relating to the evolutionary stability of AM symbiosis (14, 35). In a recent article (8), it was proposed that the mechanisms of carbon allocation that support lateral root proliferation in nutrient-rich patches might be used in symbiosis. In this way, P_i delivery by the fungus would trigger increased carbon allocation specifically to the region of the root containing the fungus (8).

We propose that the import of P_i by MtPT4 serves, either directly or indirectly, as a signal to the plant cell of the presence of a beneficial fungal symbiont. In the absence of this signal, death of the arbuscule ensues, and proliferation of the fungus is prevented. In further support of this, symbiosis does not develop under extremely low P_i conditions, and infection is stimulated dramatically with the application of small amounts of P_i (6, 36). Furthermore, although AM fungi can provide benefits other than enhanced P_i (37, 38), radioisotope experiments suggest that some symbiotic P_i transfer occurs in all AM symbioses (2). Both of these points are consistent with our proposal that P_i flow across the periarbuscular membrane is essential for symbiosis.

If, as suggested by our data, P_i delivery to the cortical cell serves as a signal to permit continued development of the arbuscule and consequently to sustain fungal existence within the root, then the plant has a robust mechanism to identify and discard an ineffective fungal symbiont before a significant commitment of resources.

Materials and Methods

Transgenic *M. truncatula* Lines. A DNA fragment corresponding to nucleotides 1363–1587 of the MtPT4 cDNA (relative to the ATG start codon) was cloned into pHellsgate 8 (39). The construct was introduced into *Agrobacterium tumefaciens* (LBA4404) and used to transform *M. truncatula* (A17) (40). Plants were transformed with the nonrecombinant pHellsgate 8 as vector controls. Primary transformants were selfed, and lines that segregated 3:1 for the presence of the *NPTII* gene ($n = 100$–120 plants) in the T2 generation were selected. Plants homozygous for a single T-DNA insertion were identified by progeny testing and the presence of the T-DNA verified by PCR.

***M. truncatula mtpt4* Mutants.** A *M. truncatula* mutant, *mtpt4-1*, was identified from an ethane mehtyl sulfonate mutant population of *M. truncatula* cv. Jemalong, genotype A17 by TILLING (41) by using FIR1 primers forward (5′-CTGGCATGGGATTCTTCACT-3′) and reverse (5′-CGGTTTCAGGCATTTTCATT-3′). The TILLING population consisted of 4,032 independently derived mutant *M. truncatula* germ lines. Mutant alleles were recovered at an average rate of one SNP per 377 germ lines per kbp interrogated, which corresponds to an average of ≈1,330 lesions per genome (germ line). *mtpt4-1* (G172R) has a G-to-A transition that alters glycine (position 172) to arginine.

Cosegregation Analysis. Individual F_2 plants (59) were assayed in parallel for the zygosity of the mutation and the *mtpt4-1* phenotype. (Details are provided in SI Fig. 9 and *SI Text*.)

Plant Growth Conditions. Unless otherwise indicated, plants were grown in a growth chamber under a 16-h-light (25°C)/8-h-dark (22°C) regime in sterile Turface (Profile Products, Buffalo Grove, IL) and inoculated with surface-sterilized *G. versiforme* spores, as described (42). Plants were fertilized twice weekly with ½ strength Hoagland's solution (43) containing 20 μM P_i. Roots were prepared for staining according to Grace and Stribley (44) and stained in 0.2 μg/ml WGA-Alexafluor 488 (Molecular Probes, Eugene, OR). Percent RLC was monitored by the modified gridline intersect method (45).

To monitor mycorrhiza-associated growth responses (Fig. 1), seedlings were planted into an acid-washed sand/Turface mixture (ratio 2:1) and inoculated with 1,000 *G. versiforme* spores. Plants were harvested at 72 dpi, weighed, and the total phosphorus level was measured according to Ames (46). To monitor development of AM symbiosis in *mtpt4-1* (reported Fig. 1 *D* and *E*), 10-day-old plants were inoculated with 800 *G. versiforme* spores and harvested at 54 dpi. To estimate extraradical hyphal length, root pieces with living hyphae attached were floated in liquid to extend the hyphae from the root. Measurements were made by using an Olympus (Melville, NY) SZX12 stereoscope. To follow arbuscule development and turnover, a synchronized inoculation system was used (32). Thirty-five-day-old plants were placed in contact with 700 *G. versiforme* spores that had received a 21-day exposure to root exudates. Plants were harvested at 49, 74, and 146 hpi and 11 dpi (three plants per line at each timepoint) and stained with WGA-Alexafluor 488. By using Metamorph software (Metamorph Universal Imaging, West Chester, PA), arbuscule size was determined by measuring the length of all visible arbuscules in independent infection units ($n = 5$ infection units for each line), with an average of 21, 42, and 66 arbuscules per infection unit at 49, 74, and 146 h, respectively. At 11 dpi, analyses were limited to observation of 28 arbuscules per infection unit. An infection unit is the infection event arising from a single entry point into the root (11). The oldest hyphae are near the appressorium and entry point, whereas the youngest hyphae are at the growing hyphal fronts (SI Fig. 11).

Staining Procedures. Vital staining was according to Schaffer and Peterson (26) followed by WGA-Alexafluor 488 staining. PolyP staining was according to Ezawa *et al.* (16).

Gene Expression Analyses. RNA extraction and RT-PCR protocols followed standard procedures. The amplification of the elongation factor EF1α was used as a control. MtPT4 primers, qMtPT4-L4 5′-GACACGAGGCGCTTTCATAGCAGC-3′; qMtPT4-R4 5′-GTCATCGCAGCTGGAACAGCACCG-3′. EF1α primers P1: 5′-GTCAAAACATGGTTGCTGCACAAGC-3′ and P2: 5′-TTAGGTCACAAGGCAGATTGCAGG-3′.

MtPT4 Immunodetection. Microsomal proteins preparation, Western blot analysis, and immunolocalization of the MtPT4 protein were performed as described (23).

Statistical Analyses. The effects of loss of MtPT4 function on shoot P, shoot growth, and arbuscule populations were tested on 5, 5, and 12 independently grown plants per line, respectively. Data were analyzed by using ANOVA to test for the effects of plant genotype on the parameters. When a significant effect was detected ($P < 0.02$), pairwise comparisons (Student's *t* test) were performed by using SAS 9.1 software (SAS Institute, Cary, NC) to identify which genotypes showed statistically significant differences ($P < 0.05$). All data presented are means ± SE, except Fig. 1*E*, where the SD is shown. The statistical significance (*P* value) is reported in the legends of the Figs. 1–5, SI Figs. 6–11, and SI Tables 1 and 2.

For analyses of arbuscule populations, arbuscules were grouped into size classes ranging from 15 to 75 μm in 10-μm increments, and for each individual infection unit, the distribution was expressed as a percentage of arbuscules in the infection unit. For the two independent vector control and MtPT4 RNAi lines, the results presented in Fig. 4 are the pooled data of individual lines 1 and 2. To fulfill the assumption of a normal distribution, the percentages were transformed by using the ARCSIN transformation before performing ANOVA.

Student's *t* test was used for other pairwise comparisons (SI Tables 1 and 2; Fig. 1 *D* and *E*).

We thank Tom Kraft for assistance with the genetic analysis of the mutants and Melina Lopez-Meyer for assistance with the setup of the arbuscule turnover experiment. Financial support for the MtPT4 project was provided by the U.S. National Science Foundation (Grant IBN-0343975, to M.J.H.). The *M. truncatula* TILLING project was supported by the U.S. Department of Agriculture (Grant CRIS 3640-21000-019-025, to D.R.C).

1. Redeker D, Kodner R, Graham L (2000) *Science* 289:1920–1921.
2. Smith SE, Smith FA, Jakobsen I (2003) *Plant Physiol* 133:16–20.
3. Newsham KK, Fitter AH, Watterson AR (1995) *J Ecol* 83:991–1000.
4. Bago B, Pfeffer PE, Shachar-Hill Y (2000) *Plant Physiol* 124:949–957.
5. Braunberger PG, Miller MH, Peterson RL (1991) *New Phytol* 119:107–113.
6. Koide R, Li M (1990) *New Phytol* 114:59–74.
7. Thomson BD, Robson AD, Abbott LK (1986) *New Phytol* 103:751–765.
8. Fitter AH (2006) *New Phytol* 172:3–6.
9. Parniske M (2004) *Curr Opin Plant Biol* 7:414–421.
10. Harrison MJ (2005) *Annu Rev Microbiol* 59:19–42.
11. Cox G, Sanders F (1974) *New Phytol* 73:901–912.
12. Bonfante-Fasolo P (1984) in *VA Mycorrhizae*, eds Powell CL, Bagyaraj DJ (CRC, Boca Raton, FL), pp 5–33.
13. Gianinazzi-Pearson V, Smith SE, Gianinazzi S, Smith FA (1991) *New Phytol* 117:61–74.
14. Smith SE, Smith FA (1990) *New Phytol* 114:1–38.
15. Cox G, Moran KJ, Sanders F, Nockolds C, Tinker PB (1980) *New Phytol* 84:649–659.
16. Ezawa T, Cavagnaro TR, Smith SE, Smith FA, Ohtomo R (2003) *New Phytol* 161:387–392.
17. Kohjima T, Saito M (2004) *Mycol Res* 108:610–615.
18. Rausch C, Daram P, Brunner S, Jansa J, Laloi M, Leggewie G, Amrhein N, Bucher M (2001) *Nature* 414:462–466.
19. Nagy F, Karandashov V, Chague W, Kalinkevich K, Tamasloukht M, Xu GH, Jakobsen I, Levy AA, Amrhein N, Bucher M (2005) *Plant J* 42:236–250.
20. Nagy R, Vasconcelos M, Zhao S, McElver J, Bruce W, Amrhein N, Raghothama K, Bucher M (2006) *Plant Biol* 8:186–197.
21. Maeda D, Ashida K, Iguchi K, Chechetka S, Hijikata A, Okusako Y, Deguchi Y, Izui K, Hata S (2006) *Plant Cell Physiol* 47:807–817.
22. Paszkowski U, Kroken S, Roux C, Briggs SP (2002) *Proc Natl Acad Sci USA* 99:13324–13329.
23. Harrison MJ, Dewbre GR, Liu J (2002) *Plant Cell* 14:2413–2429.
24. Galic S, Schneider HP, Broer A, Deitmer JW, Broer S (2003) *Biochem J* 376:413–422.
25. Chen LY, Pan CJ, Chou JY (2002) *Hum Mol Genet* 11:3199–3207.
26. Schaffer GF, Peterson LR (1993) *Mycorrhiza* 4:29–35.
27. Pearson JN, Jakobsen I (1993) *New Phytol* 124:489–494.
28. Gianinazzi-Pearson V, Gianinazzi S (1988) in *Cell to Cell Signals in Plant, Animal and Microbial Symbiosis*, eds Scannerini S, Smith DC, Bonfante-Fasolo P, Gianinazzi-Pearson V (Springer, Berlin), pp 73–84.
29. Alexander T, Toth R, Meier R, Weber HC (1989) *Can J Bot* 67:2505–2513.
30. Tamasloukht M, Sejalon-Delmas N, Kluever A, Jauneau A, Roux C, Becard G, Franken P (2003) *Plant Physiol* 131:1468–1478.
31. Akiyama K, Matsuzaki K-I, Hayashi H (2005) *Nature* 435:824–827.
32. Lopez-Meyer M, Harrison MJ (2006) in *Mol Plant–Microbe Interact*, eds Federico Sánchez CQ, López-Lara IM, Geiger O, Vol 5, pp 546–551.
33. Viereck N, Hanson PE, Jakobsen I (2004) *New Phytol* 162:783–794.
34. Ohtomo R, Saito M (2005) *New Phytol* 167:571–578.
35. Johnson NC, Graham JH, Smith AF (1997) *New Phytol* 135:575–587.
36. Bolan NS, Robson AD, Barrow NJ (1984) *Soil Biol Biochem* 16:419–420.
37. Hodge A, Campbell CD, Fitter AH (2001) *Nature* 413:297–299.
38. Govindarajulu M, Pfeffer PE, Jin HR, Abubaker J, Douds DD, Allen JW, Bucking H, Lammers PJ, Shachar-Hill Y (2005) *Nature* 435:819–823.
39. Helliwell CA, Wesley SV, Wielopolska AJ, Waterhouse PM (2002) *Funct Plant Biol* 29:1217–1225.
40. Trieu AT, Harrison MJ (1996) *Plant Cell Rep* 16:6–11.
41. McCallum CM, Comai L, Greene EA, Henikoff S (2000) *Plant Physiol* 123:439–442.
42. Liu JY, Blaylock LA, Harrison MJ (2004) *Can J Bot* 82:1177–1185.
43. Arnon DI, Hoagland DR (1940) *Soil Sci* 50:463–483.
44. Grace C, Stribley DP (1991) *Mycol Res* 95:1160–1162.
45. McGonigle TP, Miller MH, Evans DG, Fairchild GL, Swan JA (1990) *New Phytol* 115:495–501.
46. Ames BN (1966) *Methods Enzymol* 8:115–118.